ORIGINAL RESEARCH

The Induction of Pattern-Recognition Receptor Expression against Influenza A Virus through Duox2-Derived Reactive Oxygen Species in Nasal Mucosa

Hyun Jik Kim[1,2], Chang-Hoon Kim[2,3], Min-Ji Kim[4], Ji-Hwan Ryu[4], Sang Yeop Seong[3], Sujin Kim[4], Su Jin Lim[1], Michael J. Holtzman[5,6], and Joo-Heon Yoon[2,3,4,7]

[1]Department of Otorhinolaryngology, Seoul National University College of Medicine, Seoul, Korea; [5]Department of Medicine, Drug Discovery Program, Pulmonary and Critical Care Medicine, and [6]Department of Cell Biology, Washington University School of Medicine, St. Louis, Missouri; and [3]Department of Otorhinolaryngology, [2]The Airway Mucus Institute, [7]BK 21 Project for Medical Science, and [4]Research Center for Natural Human Defense System, Yonsei University College of Medicine, Seoul, Korea

Abstract

We studied the relative roles of Duox2-derived reactive oxygen species (ROS) in host defense against influenza A virus (IAV) infection in normal human nasal epithelial cells and mouse nasal mucosa. We found that Duox2 primarily generated ROS rapidly after IAV infection in normal human nasal epithelial cells and that knockdown of *Duox2* aggravated IAV infection. In addition, Duox2-derived ROS enhancement significantly suppressed IAV infection in nasal epithelium. In particular, Duox2-derived ROS were required for the induction of retinoic acid–inducible gene (RIG)-I and melanoma differentiation–associated protein 5 (MDA5) transcription. After intranasal IAV inoculation into mice, viral infection was significantly aggravated from 3 days postinoculation (dpi) in the nasal mucosa, and the IAV viral titer was highest at 7 dpi. Both RIG-I and MDA5 messenger RNA levels increased dominantly in mouse nasal mucosa from 3 dpi; consistent with this, RIG-I and MDA5 proteins were also induced after IAV infection. RIG-I and MDA5 messenger RNA levels were induced to a lower extent in the nasal mucosa of the mice that were inoculated with Duox2 short hairpin RNA, and the IAV viral titer was significantly higher in nasal lavage. Taken together, Duox2-derived ROS are necessary for the innate immune response and trigger the induction of RIG-I and MDA5 to resist IAV infection in human nasal epithelium and mouse nasal mucosa.

Keywords: influenza A virus; Duox2; reactive oxygen species; retinoic acid–inducible gene-I; melanoma differentiation–associated protein 5

Clinical Relevance

We reveal that Duox2 is responsible for reactive oxygen species (ROS)–sensitive transcription of retinoic acid–inducible gene-I and melanoma differentiation–associated protein 5 for recognition of influenza A virus (IAV) and IFN-related innate immune signaling can be induced through Duox2-derived ROS in nasal epithelium to resist IAV infection. We propose that Duox2-derived ROS are critical mediators for the antiviral innate immune mechanism and may constitute a key element in treatment or prevention of acute IAV infection in nasal epithelia.

The innate immune system of the respiratory epithelium serves as the first line of defense against invading respiratory viruses. When respiratory epithelium is exposed to viral particles, such as single- and double-stranded viral RNA, innate immune mechanisms can be activated to initiate the production of IFN, a key molecule in antiviral innate immune systems (1, 2). Initiation of these innate immune responses is achieved through the recognition of invading viruses by pattern-recognition

(Received in original form August 31, 2014; accepted in final form March 3, 2015)

This work was supported by the National Research Foundation of the Korean Government (Ministry of Science, ICT & Future Planning [MSIP]), grant 2007-0056092 (J.-H.Y.), National Research Foundation of Korea (NRF) funded by MSIP grant 2012M3A9C5048709 (J.-H.Y.), NRF funded by MSIP grant 2014R1A2A01003385 (J.-H.Y.), and the Basic Science Research Program through the NRF funded by Ministry of Education, Science, and Technology grant 2013R1A1A2011612 (H.J.K.).

Author Contributions: conception and design—H.J.K. and J.-H.Y.; analysis of data—C.-H.K., M.-J.K., J.-H.R., and S.Y.S.; interpretation of data—H.J.K., S.K., and S.J.L.; research advice—M.J.H.; drafting the manuscript for important intellectual content—H.J.K.

Correspondence and requests for reprints should be addressed to Joo-Heon Yoon, M.D., Ph.D., Department of Otorhinolaryngology, Yonsei University College of Medicine, 50 Yonsei-ro, Seodaemun-gu, Seoul 120-752, Korea. E-mail: jhyoon@yuhs.ac

This article has an online supplement, which is accessible from this issue's table of contents at www.atsjournals.org

Am J Respir Cell Mol Biol Vol 53, Iss 4, pp 525–535, Oct 2015

Originally Published in Press as DOI: 10.1165/rcmb.2014-0334OC on March 9, 2015
Internet address: www.atsjournals.org

receptors (PRRs), and virus-derived nucleic acids are considered to activate various PRRs, including members of the membrane-bound Toll-like receptor (TLR) family, such as TLR3, -7, and -9, and the recently identified cytoplasmic retinoic acid–inducible gene (RIG)-I–like receptors (RLRs), including RIG-I and melanoma differentiation–associated protein 5 (MDA5) (3). After the recognition of viral RNAs, the antiviral innate immune response is activated, mainly through the rapid expression of IFNs in nasal epithelium (4). IFNs secreted after viral infection induce antiviral innate immune responses via the Janus kinase/signal transducer and activator of transcription signaling pathway, which facilitates intracellular antiviral signaling through the induction of more than 300 IFN-stimulated genes (4). Reportedly, rapid production of IFN-stimulated genes could actually be associated with degradation of viral RNA, preventing virus translation and virion assembly, and suppressing viral replication (5, 6).

Influenza A virus (IAV) is a highly contagious agent that causes upper and lower respiratory tract infection, and exhibits tremendous genetic variability through continuous mutations (7). Accordingly, novel influenza strains regularly evolve, to which humans have little immunity, resulting in global pandemics. For this reason, the cure rate of IAV-related pulmonary infectious diseases has not been changed over the last years. Therefore, more research is needed to control IAV infection in the respiratory tract, and the identification of new therapeutic inductors represents a critical research goal.

Reactive oxygen species (ROS) are believed to be inevitable toxic by-products that cause cellular damage or stress (8). However, mounting evidence suggests that ROS generation is an important component of the host's arsenal to combat invading microorganisms (9–11). The most common free radical in biological systems is superoxide anion and hydrogen peroxide, products of various oxidative enzymes, including nicotinamide adenine dinucleotide phosphate oxidase (Nox). Seven isoforms of Nox (Nox1, Nox2, Nox3, Nox4, Nox5, Duox1, and Duox2) have been identified in humans, and Duox has been shown to be the major Nox isoform involved in ROS generation in airway epithelium (8–10). Furthermore, interesting lines of research describe Duox-mediated ROS generation as an integral part of the host defense system at mucosal surfaces (10, 12, 13). Recently, it has been verified that Duox2 is primarily responsible for protection against viral invaders and plays an important role in antiviral innate immunity (14). However, the distinct relationship between Duox2-derived ROS and IFN-related innate immune responses is not fully understood.

Here, we used normal human nasal epithelial (NHNE) cells and an *in vivo* model to clarify the role of Duox2 in acute IAV infection, and investigated how Duox2-derived ROS are responsible for antiviral defense mechanisms. Our data suggest that Duox2 is critical for the generation of key cell surface viral recognition molecules/PRRs and serves as a host-protective immune response to control acute viral infection in nasal mucosa.

Materials and Methods

More detailed Materials and Methods may be found in the online supplement.

Cell Culture

The Institutional Review Board (IRB) of the Chung-Ang University College of Medicine approved this study (IRB number C20122095) and all subjects who participated in the study provided written informed consent. Specimens for the culture of NHNE cells were obtained from the middle nasal turbinate of five healthy volunteers. We cultured these specimens using a system designed for NHNE cells (14–16). Briefly, passage-2 NHNE cells (1×10^5 cells/culture) were seeded in 0.5-ml culture medium on Transwell clear culture inserts (24.5 mm; 0.45-μm pore size; Costar Co., Cambridge, MA). Cells were cultured in a 1:1 mixture of basal epithelial growth medium and Dulbecco's modified Eagle's medium containing previously described supplements. All the experiments described herein used NHNE cells at 14 days after air–liquid interface formation.

Mice

Male C57BL/6J (B6) mice (Orientalbio, Seoul, Korea) aged 7 weeks (19–23 g) were used as wild-type (WT) and maintained in our animal facilities under specific, pathogen-free conditions. *In vivo* experiments were approved by the IRB of the Yonsei University College of Medicine (IRB number 2014-0163).

Virus Inoculation

NHNE cells were either mock-infected (PBS) or inoculated with IAV (WS/33, H1N1) at a multiplicity of infection (MOI) of 1. IAV (WS/33, H1N1; 213 pfu in 30 μl PBS) was inoculated into mice by intranasal delivery.

Real-Time PCR

Total RNA was isolated from NHNE cells and homogenized mouse nasal mucosa infected with WSN/33 (H1N1) at 10 and 30 minutes, 1, 2, and 8 hours, and 1, 2, 3, 7, 10, and 14 days using TRIzol (Invitrogen, Carlsbad, CA). Complementary DNA (cDNA) was synthesized from 3 μg of RNA with random hexamer primers using Moloney murine leukemia virus reverse transcriptase (PerkinElmer Life Sciences, Waltham, MA and Roche Applied Science, Indianapolis, IN).

The Measurement of ROS

After stimulation with WS/33 (H1N1) for 1 hour, confluent cells were washed with RPMI (lacking phenol red). The cells were washed with 1 ml of Hanks' balanced salt solution at least five times to remove mucus secretion, and were then incubated with 5 μM of 2′,7′-dichlorofluorescein diacetate (DCF-DA) for 10 minutes. Transwell clear culture inserts were examined with a Zeiss Axiovert 135 inverted microscope equipped with a 20× Neofluor objective and a Zeiss LSM 410 confocal attachment (Zeiss, Minneapolis, MN).

Cell Transfection with Nox4, Duox1, and Duox2 Short Hairpin RNAs

Expression of Nox4, Duox1, and Duox2 was suppressed using gene-specific short hairpin RNA (shRNA) (lentiviral particles; Santa Cruz Biotechnology, Dallas, TX), and the transfection rates for shRNAs were determined to be greater than 70% in NHNE cells. The cells were transfected with each shRNA using the Oligofectamine reagent following the manufacturer's instructions (Invitrogen). The shRNA (10 μl, 1×10^4 infectious units of virus) and Oligofectamine (1 μg) were mixed individually with the culture media.

Duox2 Overexpression Using Full-Length of cDNA Clones

For Duox2 overexpression in NHNE cells, cells were transfected with the Duox2 (NM_177610) and Duoxa2 (NM_025777) mouse cDNA ORF Clones purchased from Origene (Beijing, China).

Duox2 Silencing Using Lentiviral shRNA in Mouse Nasal Mucosa

For Duox2 silencing in mouse nasal mucosa using shRNA lentiviral particles (Thermo Fisher Scientific Inc, Waltham, MA), mice were anesthetized with 50 mg/kg Zoletil (Virbac Korea, Seoul, Korea) and 10 mg/kg Rompun (Bayer AG, Leverkusen, Germany) and given either mouse Duox2 shRNA (clone ID V3LMM-425530) or scrambled shRNA lentiviral particle (3×10^7 TU/ml) twice 3 days apart, intranasally in a total volume of 30 μl (17). After 6 days, the mice were used for the experiments.

Statistical Analysis

At least three independent experiments were performed with cultured cells from each donor, and the results are presented as the mean value (±SD) of triplicate cultures. Differences between treatment groups were evaluated by ANOVA with a *post hoc* test. Differences were considered significant at P less than 0.05.

Results

NHNE Cells Were Susceptible to IAV Infection

NHNE cells were obtained from five healthy subjects to assess the susceptibility to IAV and were infected with IAV WS/33 (H1N1) at an MOI of 1. Supernatants and cell lysates were harvested at 10 and 30 minutes, 1, 2, and 8 hours, and 1, 2, and 3 days postinoculation (dpi). We then measured the messenger RNA (mRNA) levels of IAV using real-time PCR and found that IAV mRNAs increased significantly from 1 day after infection (mean IAV mRNA: 1.2×10^5 (1 dpi); 1.8×10^6 (2 dpi); 2.2×10^6 (3 dpi); $P < 0.05$; Figure 1A). We examined viral titer of IAV by plaque assay and found that viral titer also increased significantly from 1 dpi (2.2×10^5 pfu/ml). Peak titer of IAV was 1.2×10^6 pfu/ml at 3 days after infection ($P < 0$; Figure 1B). These findings demonstrate the susceptibility of the nasal epithelium to WS/33 (H1N1), and show that the mRNA level and viral titer of IAV increased from 1 day after IAV infection.

Duox2-Derived ROS Are Required for Controlling IAV Infection

We reported that IAV infection induced intracellular ROS generation at 1 hour postinoculation (hpi) and verified that *Nox4*, *Duox1*, and *Duox2* mRNA levels increased significantly after IAV infection in nasal epithelium, and the mRNA levels of *Nox1*, *Nox2*, *Nox3*, and *Nox5* were minimally induced by IAV infection (14). Based on these findings, we focused on Nox4, Duox1, and Duox2 as possible Nox subtypes that are involved in IAV-induced ROS generation in nasal epithelium. We then measured the mRNA levels of *Nox4*, *Duox1*, and *Duox2* using real-time PCR and observed that the mRNA levels of these Nox enzymes increased considerably from 10 minutes after infection and were maximal at 30 minutes (*Nox4* mRNA, 32.0 ± 1.1 fold over control; *Duox1* mRNA, 19.4 ± 1.4 fold over control; *Duox2* mRNA, 19.1 ± 0.8 fold over control; $P <$ 0.05; Figures 2A–2C) after IAV infection in NHNE cells.

NHNE cells were transfected with Nox4, Duox1, and Duox2 shRNA to suppress the endogenous mRNA expression of each Nox subtype, and ROS levels were then measured using a fluorescence-based assay with 2′,7′-DCF-DA. Then, plaque assay and Western blot analysis were performed to measure the viral titer and IAV nucleoprotein (NP). We found that intracellular ROS generation at 1 hour after IAV infection was significantly attenuated in the cells that were transfected with Duox2 shRNA, and the amount of intracellular ROS was not changed in cells

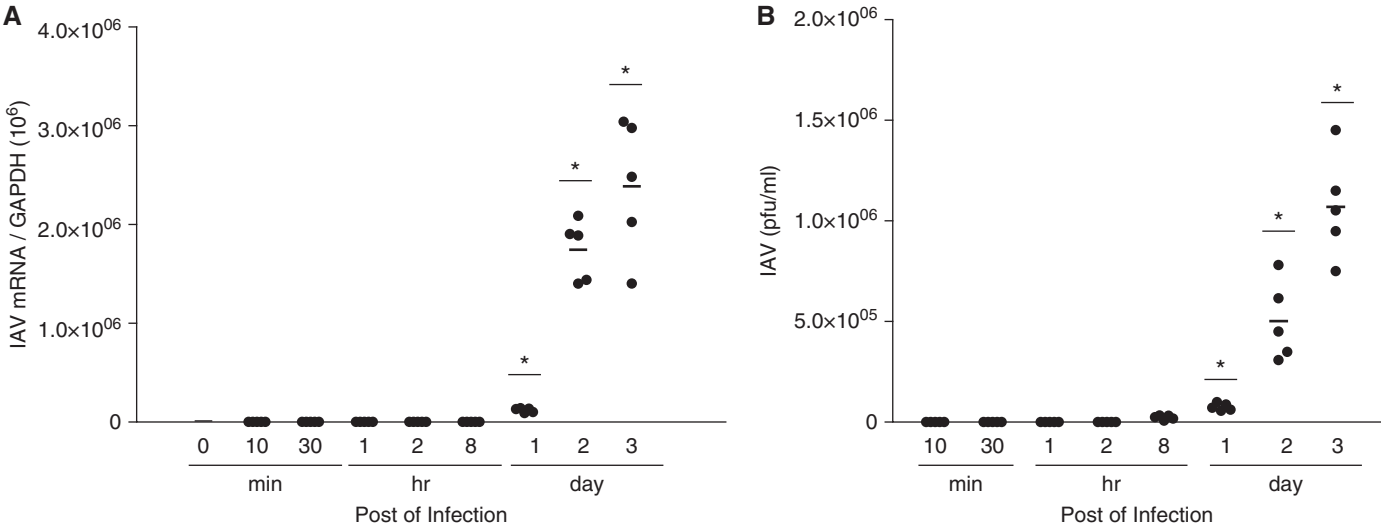

Figure 1. Normal human nasal epithelial (NHNE) cells were susceptible to influenza A virus (IAV) infection. NHNE cells from five healthy volunteers were inoculated with WS/33 (H1N1) for 10 and 30 minutes, 1, 2, and 8 hours, and 1, 2, and 3 days at an multiplicity of infection (MOI) of 1. (*A*) Real-time PCR showed that the IAV messenger RNA (mRNA) level was elevated from 1 day postinoculation (dpi) and was highest at 3 dpi. (*B*) Plaque assay also showed that viral titer was significantly higher from 1 dpi. Results are presented here as the mean ± SD from five independent experiments. *$P < 0.05$ compared with levels in mock-infected cells. GAPDH, glyceraldehyde 3-phosphate dehydrogenase.

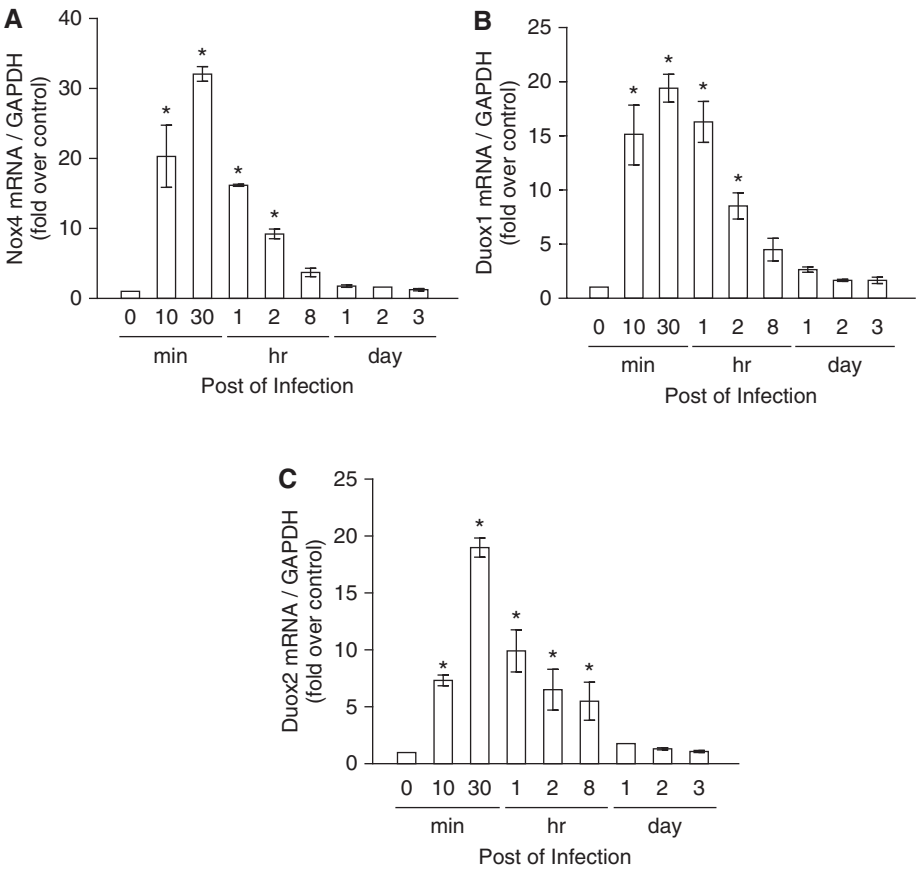

Figure 2. The mRNA levels of three nicotinamide adenine dinucleotide phosphate oxidase (Nox) subtypes are preferentially induced to produce reactive oxygen species (ROS) after IAV infection. NHNE cells were inoculated with WS/33 (H1N1) for 10 and 30 minutes, 1, 2, and 8 hours, and 1, 2, and 3 days at an MOI of 1. Real-time PCR showed that Nox4 (*A*), dual oxidase (Duox) 1 (*B*), and Duox2 (*C*) mRNA levels are induced from 10 minutes after infection. Results are presented here as the mean ± SD from five independent experiments. *$P < 0.05$ compared with mRNA levels in mock-infected cells.

transfected with Nox4 and Duox1 (Figure 3A). IAV viral titers in cells (5.9×10^6 pfu/ml) that had been transfected with Duox2 shRNA before IAV infection were significantly higher after infection compared with IAV-infected cells (2.2×10^6 pfu/ml), cells transfected with control shRNA, cells transfected with Nox4 shRNA, and cells transfected with Duox1 shRNA before IAV infection (Figure 3B). In addition, Western blot analysis also revealed that IAV NP expression showed a more considerable increase in Duox2 knockdown cells than in cells showing normal Duox2 expression (Figure 3C).

Subsequently, we transfected the cDNA clones containing the entire pCMV-Duox2 and Duoxa2 sequences into NHNE cells for the enhancement of Duox2-derived ROS. RT-PCR showed that both Duox2 and Duoxa2 mRNA levels were effectively elevated (Figure 3D) and the amount of intracellular ROS was significantly higher in cells overexpressing Duox2 and Duoxa2 at 1 hpi (Duox2 overexpression with IAV infection, 58.9 ± 4.6; only Duox2 overexpression, 24.7 ± 2.7; IAV infection, 33.5 ± 1.2; versus control 5.8 ± 1.6; $P < 0.05$; Figure 3E). Interestingly, increased IAV mRNA level (3.6×10^5 versus 3.9×10^4; $P < 0.05$; Figure 3F) and NP expression (Figure 3G) at 2 dpi was significantly attenuated in NHNE cells overexpressing Duox2 and Duoxa2. These results indicate that Duox2 is a key mediator, critically important for the generation of ROS and viral load attenuation in NHNE cells. Attenuation of Duox2-derived ROS generation subsequently aggravated acute IAV infection, and IAV infection could be effectively controlled if the amount of Duox2-derived ROS was increased in the nasal epithelium.

TLR3, RIG-I, and MDA5 Are Responsible for Recognition of IAV in NHNE Cells

To further evaluate the potential role of Duox2-derived ROS at 1 hpi after IAV infection in nasal epithelium, we examined the relationship between Duox2-derived ROS and the transcription of PRRs after IAV infection.

We infected NHNE cells with WS/33 (H1N1) at an MOI of 1, and the cell lysates were harvested at 1, 2, and 3 dpi. We then measured the mRNA levels of PRRs, such as TLR3, TLR7, TLR9, RIG-I, and MDA5, which are known to sense double-stranded RNA virus in the respiratory epithelium. The results showed that *TLR3*, *RIG-I*, and *MDA5* mRNA levels were significantly induced from 1 dpi, and these levels were maintained up to 3 dpi (Figure 4A). To analyze this in more detail, we determined the levels of transcription for *TLR3*, *RIG-I*, and *MDA5* after IAV infection using real-time PCR. Increased *TLR3*, *RIG-I*, and *MDA5* gene expression levels were observed from 8 hpi with a peak at 1 dpi (TLR3, 969,121.4 ± 551,543.3; RIG-I, 3,290,121.5 ± 282,842.7; MDA5, 1,214,512.3 ± 34,648.2; Figures 4B–4D). These data suggest that TLR3, RIG-I, and MDA5 are the dominant PRRs responding to IAV infection, as such are critical components of the innate immune response in nasal epithelium.

Duox2-derived ROS Are Involved in RIG-I– and MDA5-Mediated Immune Response

To determine the relationship between Duox2-derived ROS and induction of TLR3, RIG-I, and MDA5 transcription after IAV infection, cells were transfected with Duox2 shRNA and then inoculated with IAV WS/33 (H1N1). The mRNA levels of *TLR3*, *RIG-I*, and *MDA5* were analyzed by real-time PCR at 1 dpi. IAV infection resulted in increased mRNA levels of *TLR3*, *RIG-I*, and *MDA5* at 1 dpi, and IAV-induced *RIG-I* and *MDA5* mRNA levels decreased significantly in cells with knocked-down Duox2 gene expression compared with cells transfected with control shRNA (RIG-I, 1.3×10^6 versus 5.1×10^5; MDA5, 3.3×10^6 versus 1.2×10^6; $P < 0.05$). However, *TLR3* mRNA levels were not attenuated in Duox2 knockdown cells (Figures 5A–5C).

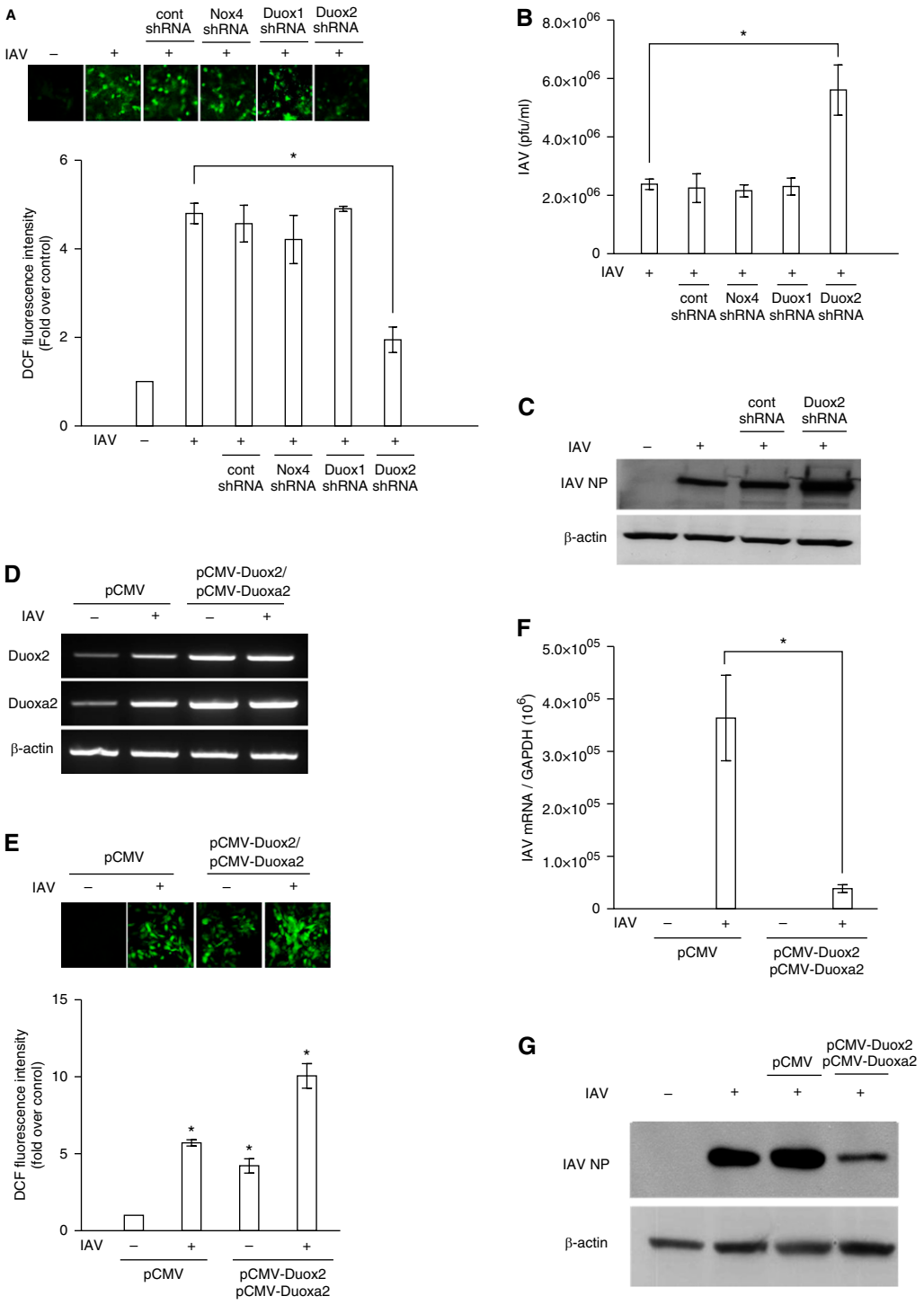

Figure 3. Duox2 is mainly involved in IAV-induced intracellular ROS generation in the nasal epithelium. NHNE cells were transfected with control (Cont) short hairpin RNA (shRNA), Nox4 shRNA, Duox1 shRNA, and Duox2 shRNA to suppress endogenous mRNA expression for 48 hours, and plaque assay was performed to measure changes in IAV viral titers after the suppression of Nox4-, Duox1-, and Duox2-induced intracellular ROS generation (*A* and *B*). After transfecting control shRNA and Duox2 shRNA into NHNE cells, Western blot analysis was performed to measure changes in IAV nucleoprotein (NP) after the suppression of Duox2-derived intracellular ROS generation (*C*). NHNE cells were transfected with pCMV-Duox2 and Duoxa2 overexpression vectors to enhance Duox2-derived intracellular ROS. RT-PCR showed that both Duox2 and Duoxa2 mRNA levels were significantly induced (*D*), and the amount of intracellular ROS also increased (*E*) after transfection with Duox2 and Duoxa2 overexpression vectors. Plaque assay and Western blot analysis were performed to measure changes in IAV viral titers (*F*) and IAV NP (*G*) after the enhancement of Duox2-derived intracellular ROS. The fluorescence intensity and Western blot analysis data are representative of five independent experiments, and results are presented here as the mean ± SD from five independent experiments. $^*P < 0.05$ compared with levels in IAV-infected cells or cells transfected with control shRNA or pCMV vector. DCF, 2′,7′-dichlorofluorescein.

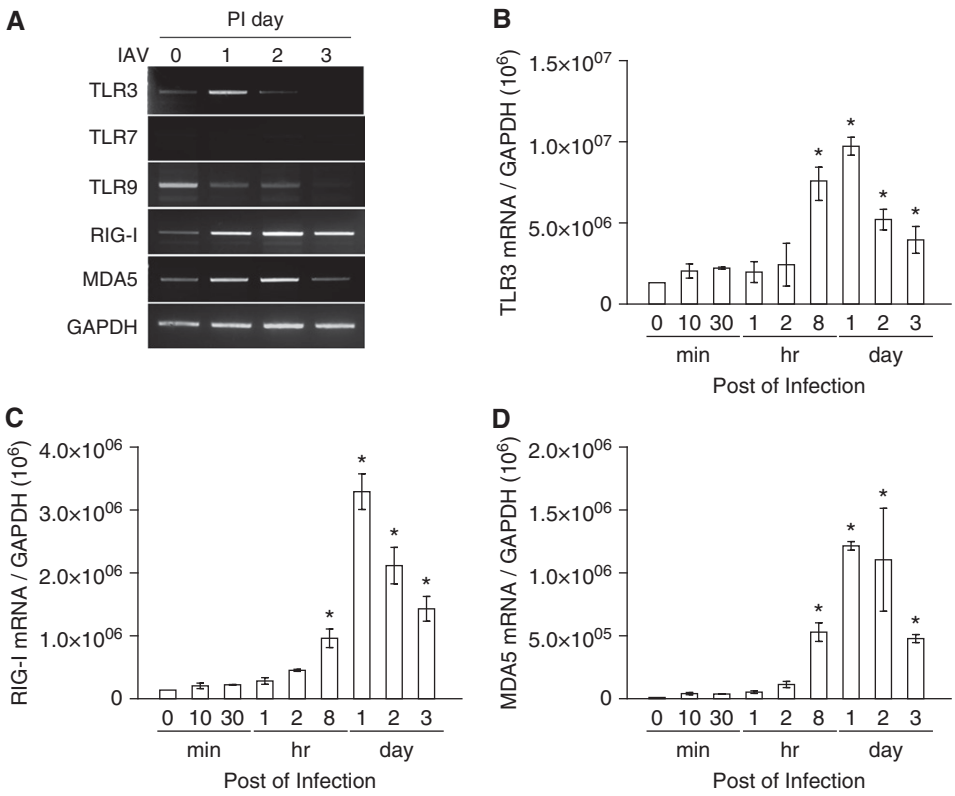

Figure 4. The mRNA levels of Toll-like receptor (TLR) 3, retinoic acid–inducible gene (RIG)-I, and melanoma differentiation–associated protein 5 (MDA5) are preferentially induced to recognize IAV in nasal epithelium. NHNE cells were inoculated with WS/33 (H1N1) for 10 and 30 minutes, 1, 2, and 8 hours, and 1, 2, and 3 days, at an MOI of 1. RT-PCR (*A*) and real-time PCR showed that TLR3 (*B*), RIG-I (*C*), and MDA5 (*D*) mRNA levels are induced from 8 hours after infection. Results are presented here as the mean ± SD from five independent experiments. *$P < 0.05$ compared with mRNA levels in mock-infected cells. PI day, postinfection day.

In addition, both *RIG-I* and *MDA5* mRNA levels were considerably elevated in cells with an increased amount of Duox2-derived ROS compared with cells that were infected with IAV (RIG-I, 4.3×10^6 versus 2.5×10^6; MDA5, 5.6×10^6 versus 2.4×10^5; $P < 0.05$; Figures 5D and 5E). Interestingly, both *RIG-I* and *MDA5* mRNA levels were significantly higher in Duox2-overexpressing cells without IAV infection than in uninfected cells (RIG-I, 6.1×10^6 versus 1.2×10^5; MDA5, 7.4×10^6 versus 1.0×10^5; $P <$ 0.05). These results provide strong evidence that Duox2-derived ROS are essential for the induction of cytoplasmic PRRs, RIG-I, and MDA5 in nasal epithelium.

Duox2-derived ROS Are Required for Induction of RIG-I and MDA5 in Nasal Mucosa *In Vivo*

To prove whether Duox2 was involved in the induction of RIG-I and MDA5 in nasal mucosa in response to IAV infection, we established an *in vivo* model of acute nasal IAV infection in mice. First, we infected B6 mice ($n = 3$) with IAV WS/33 (H1N1), via the intranasal administration of a dose of 213 pfu. As a gross determinant of virus-induced morbidity, the body weights of the infected WT mice were monitored for 14 days and significant weight loss values were observed from 6 dpi until 12 dpi compared with uninfected mice (Figure 6A). Then we inoculated 213 pfu IAV WS/33 (H1N1) to B6 mice ($n = 5$) by intranasal delivery and performed the plaque assay using nasal lavage (NAL) fluid, which was obtained at 3, 7, 10, and 14 dpi. The results showed that viral titer was elevated significantly from 3 dpi, and the highest titer was observed at 7 dpi (14,200 pfu/ml). Subsequently, the viral titer gradually decreased until 14 dpi (2,500 pfu/ml) in IAV-infected mice (Figure 6B). Correspondingly, hematoxylin and eosin–stained micrographs of coronal nose sections were obtained from WT mice at 0, 7, and 14 dpi; mouse nasal mucosa from 7 dpi revealed severe subepithelial consolidation, larger amount of secretion in nasal cavity, and increased epithelium detachment compared with nasal mucosa from mice at 0 dpi (Figure 6C). In particular, polymorphonuclear neutrophil infiltration was dominantly in nasal mucosa at 7 dpi (Figure 6D). These pathological findings were not observed in the nasal mucosa from mice at 14 dpi. Based on these findings, we conclude that mouse nasal mucosa is susceptible to IAV and that infection is significant as early as 3 dpi. IAV infection reached its peak on Day 7 and then declined until Day 14 in mice with normal immune responses.

Finally, we attempted to determine if differentially Duox2-generated ROS were related to the induction of RIG-I and MDA5 in response to IAV infection. For this study, we transfected both control shRNA ($n = 5$, control short hairpin RNA [shCont] mice) and Duox2 shRNA ($n = 5$, shDuox2 mice) lentiviral particles by intranasal

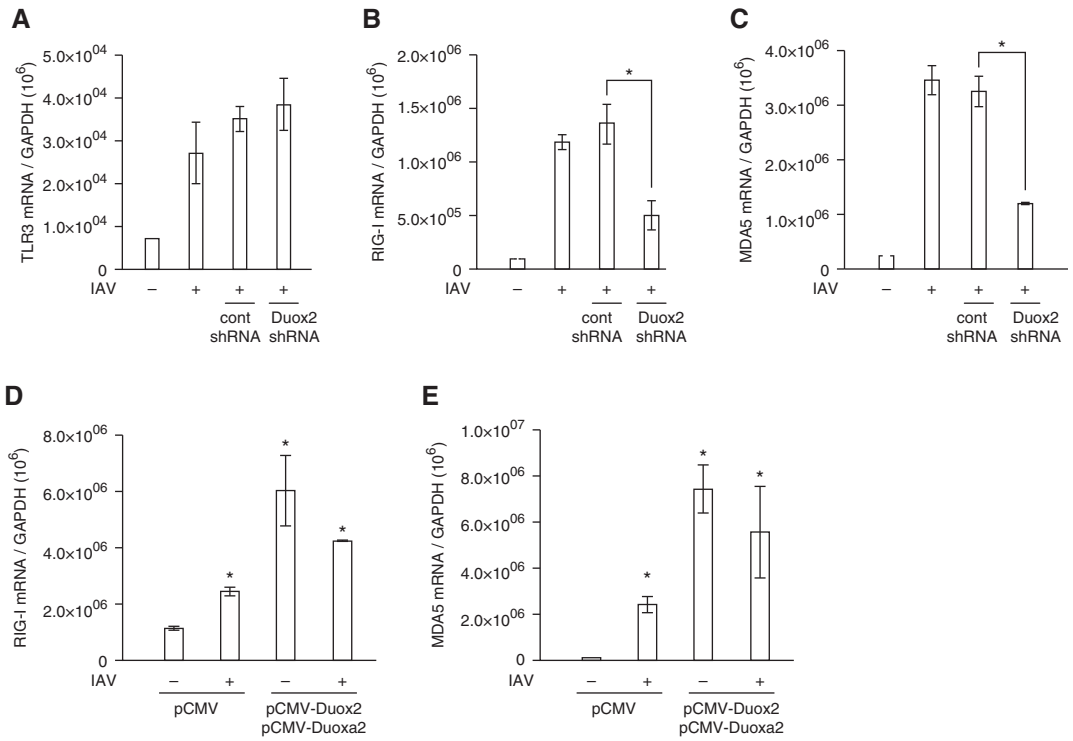

Figure 5. The transcription of RIG-I and MDA5 is preferentially augmented by Duox2-derived ROS after IAV infection. NHNE cells were transfected with control shRNA and Duox2 shRNA, and real-time PCR was performed to measure changes in IAV-induced TLR3 (*A*), RIG-I (*B*), and MDA5 (*C*) gene expression. IAV-induced RIG-I and MDA5 mRNA levels were significantly attenuated in cells transfected with Duox2 shRNA. IAV-induced TLR3 mRNA levels were not changed after the suppression of Duox2-derived intracellular ROS in NHNE cells. The gene expression levels of both RIG-I (*D*) and MDA5 (*E*) were considerably elevated in cells in which Duox2-derived ROS levels were increased through the use of Duox2 and Duoxa2 overexpression vectors. The results are presented here as the mean ± SD from five independent experiments. *$P < 0.05$ compared with levels in IAV-infected cells or cells transfected with control shRNA or pCMV vector.

challenge twice, 3 days apart, and then inoculated 213 pfu IAV WS/33 (H1N1) into mice by intranasal delivery. We did not observe any difference in the survival rate between shCont mice, shDuox2 mice, and WT mice before IAV infection. However, this was accompanied by a significant decrease in survival rate of shDuox2 mice after IAV infection. Endogenous *Duox2* gene expression on nasal mucosa was decreased by 78% after Duox2 shRNA transfection (shCont mice, 2.8×10^5, versus shDuox2 mice, 5.9×10^4; $P < 0.05$) and the survival rate of mice transfected with Duox2 shRNA after IAV infection was significantly lower than that of shCont mice at 12 dpi (Figures 7A and 7B). This was accompanied by a significant increase in the mean IAV mRNA level from mouse nasal mucosa (shDuox2 mice, 2.3×10^7, versus shCont mice, 5.4×10^6; $P < 0.05$; Figure 7C) and in the viral titer from NAL fluid (shDuox2 mice, 2.2×10^6, versus shCont mice, 4.7×10^5; $P < 0.05$; Figure 7D) at 7 dpi. These data reveal that Duox2 participates in the overall host defense of mouse nasal mucosa during the early stages of IAV infection.

After inoculating B6 mice ($n = 5$) with 213 pfu IAV WS/33 (H1N1) by intranasal delivery, cell lysates from nasal mucosa were harvested at 0, 3, 7, 10, and 14 dpi. We then measured the mRNA levels of *TLR3*, *TLR7*, *TLR9*, *RIG-I*, and *MDA5* using real-time PCR and found that the mRNA levels of both *RIG-I* and *MDA5* increased significantly from 3 dpi (RIG-I, 9.9×10^4 versus 8.8×10^3; MDA5, 3.1×10^5) compared with nasal mucosa from uninfected mice (RIG-I, 8.8×10^3; MDA5, 9.1×10^3; $P < 0.05$; Figure 7E). The mRNA levels of *TLR3*, *TLR7*, and *TLR9* were minimally enhanced by IAV inoculation (Figure 7E). The protein expression of both RIG-I and MDA5 were also induced at 3 dpi in cell lysates from mouse nasal mucosa (Figure 7F).

Next, RIG-I and MDA5 gene and protein expression levels were measured with cell lysates from the nasal mucosa of shDuox2 mice and compared with shCont mice. The results revealed that IAV-induced gene expression levels of *RIG-I* (shCont mice, 5.5×10^5; shDuox2 mice, 7.6×10^4; $P < 0.05$) and *MDA5* (shCont mice, 1.4×10^6; shDuox2 mice, 3.9×10^5; $P < 0.05$; Figure 7G), as well as their protein expression levels, were significantly attenuated in the nasal mucosa of shDuox2 mice (Figure 7H). These results suggest that RIG-I and MDA5 are dominant receptors for IAV recognition, and that Duox2 might be essential for the induction of RIG-I and MDA5 expression levels in mouse nasal mucosa.

Discussion

We found that Duox2 is the dominant source of ROS in response to IAV infection,

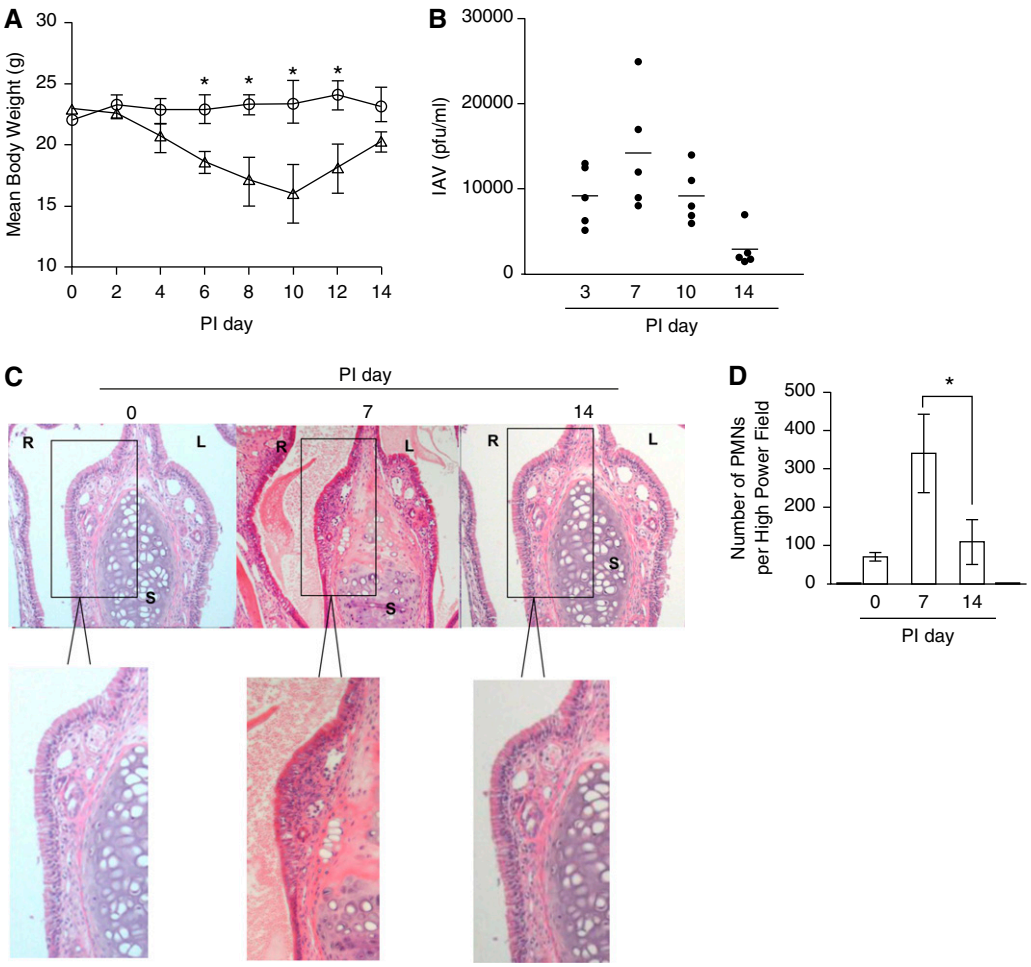

Figure 6. IAV infection *in vivo*. Wild-type (WT) mice were infected with 213 pfu IAV WS/33 (H1N1) and assessed for loss of body weight (*A*) (*circles*, no infection mice, $n = 3$; *triangles*, infection mice, $n = 3$, $^*P < 0.05$ compared with mean body weight of no infection mice) and viral titer from nasal lavage (NAL) fluid of infected mice ($n = 5$) (*B*) over the postinfection period (the results are presented here as the mean ± SD from the NAL fluid from five mice). Hematoxylin and eosin (H&E) micrographs of nose (coronal) sections obtained from WT mice infected with 213 pfu IAV on Days 0, 7, and 14. The H&E micrographs are representative of nose sections from five mice (*C*) and polymorphonuclear neutrophils (PMNs) were counted in subepithelium of nasal mucosa (*D*). $^*P < 0.05$ compared the number of PMNs in nasal mucosa of mice at PI 7 and PI 14. R, right; L, left; S, septum. *Boxed areas* in *C* are shown enlarged in bottom images.

and Duox2-derived ROS are integral mediators of transcription of RLR family genes, including RIG-I and MDA5, which are major components of IAV recognition receptors in the nasal epithelium (Figure 8).

In the respiratory tract, ROS are regarded as one of the pathological components of chronic inflammatory airway diseases, such as asthma, pneumonia, and chronic obstructive pulmonary disease (18–20). Based on this knowledge, some researchers have suggested that faster clearance of ROS could reduce lung damage and improve lung function (21, 22). However, ROS have recently been shown to function as messengers, influencing a variety of immunological processes and enhancing host immunity through prevention of pathogen-induced proinflammatory cytokines (23–25). ROS generation by exogenous pathogens has also been established in respiratory epithelial cells, and modulation of ROS was reported to be important for respiratory virus–induced innate immune mechanisms (8, 9, 14). In the present study, we showed that IAV infection increased ROS generation in the human nasal epithelium and IAV infection was aggravated when the functions of enzymes that result in ROS generation were clearly knocked down. Therefore, we aimed to assess how ROS contributed to the immune response against IAV infection in nasal epithelium. We demonstrated that IAV-induced ROS were involved in the activation of IAV recognition receptors, especially RIG-I and MDA5, and scavenging of ROS suppressed the transcription of both receptors after IAV infection in the nasal epithelium. The current findings suggest that the absence of ROS could lead to accelerated IAV infection by impeding the transcription of viral recognition receptors in nasal epithelium. Although little is known about the regulatory mechanisms behind RLRs in the nasal epithelium, we conclude that IAV-induced ROS might be a critical mediator for RIG-I and MDA5 transcription in

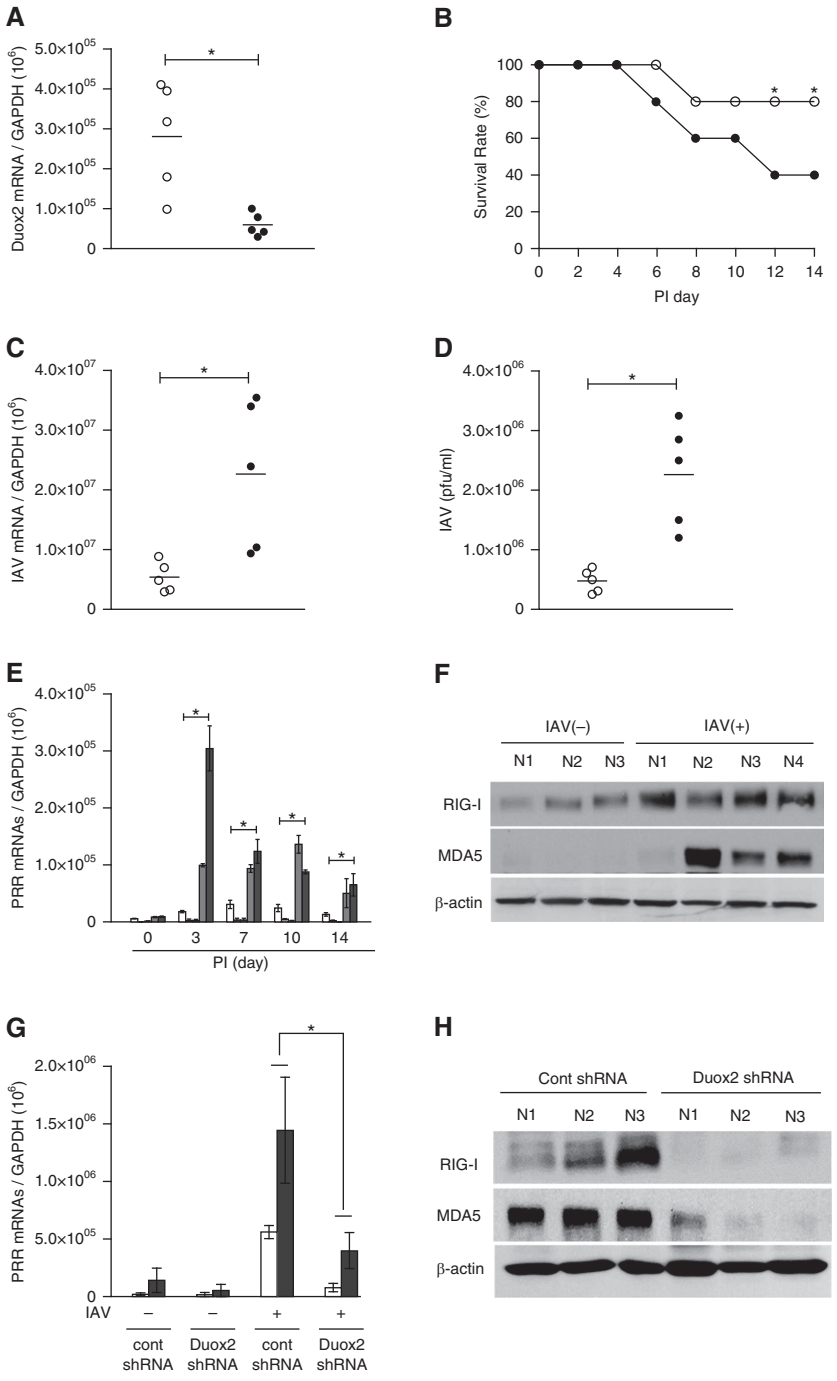

Figure 7. IAV infection is enhanced in Duox2 mutant mice, and Duox2-induced ROS are required for inducing IAV recognition receptors. WT mice were pretreated with control shRNA (shCont; $n = 5$) or Duox2 shRNA (shDuox2; $n = 5$) mice, and mice infected with 213 pfu IAV WS/33 (H1N1) were assessed for *Duox2* gene expression on nasal mucosa (*A*) and survival rate over the postinfection period (*B*). Cell lysates from mice nasal mucosa and NAL fluid were obtained at 7 dpi, and real-time PCR and plaque assays were performed to compare viral mRNA levels (*C*) or viral titers (*D*) between shCont mice and shDuox2 mice (*open circle*, shCont mice; *solid circle*, shDuox2 mice). WT mice ($n = 5$) infected with 213 pfu IAV WS/33 (H1N1) were assessed for mRNA levels of TLR3, TLR7, TLR9, RIG-I, and MDA5, and cell lysates of mouse nasal mucosa and NAL fluid were obtained at 3, 7, 10, and 14 dpi (*E*) (*white bar*, TLR3; *light gray bar*, TLR7; *gray bar*, TLR9; *dark gray bar*, RIG-I; *black bar*, MDA5). Real-time PCR showed that both RIG-I and MDA5 mRNA levels were significantly induced after IAV infection in the

controlling IAV replication. Therefore, further research on the enzymatic source of IAV-induced ROS generation may promote a greater understanding of the RLR-mediated innate immune response and suggest better therapeutic strategies for acute IAV infection in nasal epithelium.

In particular, the importance of Nox enzymes in innate host defense is exemplified by the role of Nox2 in the generation of high amounts of ROS in phagocytic cells, as part of an antibacterial mechanism. However, Duox has been widely appreciated as a critical component for ROS production in the lungs (9, 26–29), and evidence points to Duox as the main Nox isoform that generates ROS in the apical portion of bronchial epithelial cells (30, 31). We also previously reported that Duox is the most abundant Nox subtype in human nasal epithelium (10). Recent studies suggest that Duox may participate in innate host defense, and also appears to be involved in protective cellular signaling in response to a defined danger signal, performed by an intracellular NOD-like receptor system, such as NOD2-mediated antibacterial responses (13, 32). A direct contribution of Duox-derived ROS to the early steps of antiviral host defense has also been reported, and Duox-derived ROS has been shown to reduce the alternative splicing of influenza viral gene segments and cause decreased release of viral particle (33). In the present study, we found that Duox2 is a dominant enzyme in ROS generation after IAV infection in nasal epithelia. In particular, knockdown of Duox2 could aggravate IAV infection in nasal epithelium, and the innate immune response would be stronger in Duox2-overexpressed cells. Duox2 gene expression was elevated rapidly after IAV infection, and ROS production was initiated to activate viral recognition receptors. We suggest that suppression of Duox2-derived ROS or reduction of Duox2 expression inactivates a series of RLR family genes, leading to deterioration of IAV infection. In contrast, overexpression of Duox2 increased ROS generation and enhanced both RIG-I and MDA5 transcription, resulting in activation of the innate immune response against IAV infection in nasal epithelium.

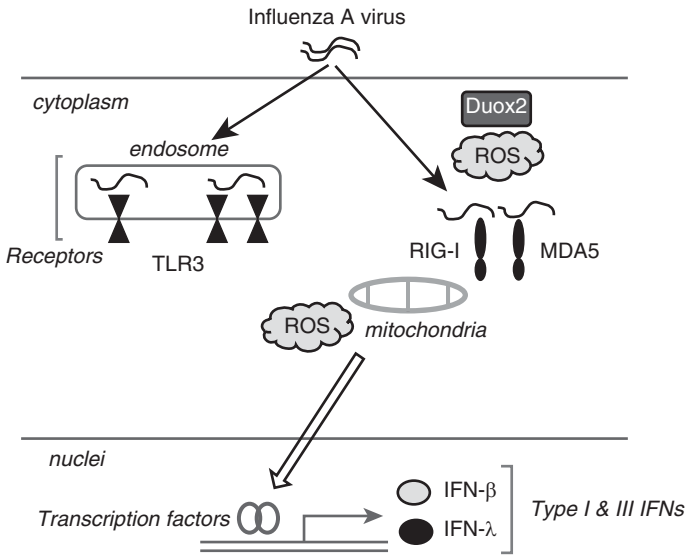

Figure 8. Schematic picture of the innate immune response against IAV infection in nasal epithelial cells. IAV infection triggers Duox2-derived and mitochondrial ROS generation, resulting in mediating IFN-β and λ secretion in NHNE cells. In particular, Duox2-derived ROS are primarily involved in the rapid induction of IAV recognition receptors, especially RIG-I and MDA5, and Duox2-derived ROS would be necessary for IAV sensing in human nasal epithelium.

The precise molecular patterns of virus replication recognized by RIG-I and MDA5 have been reported, and the elucidation of a role for the RLRs in virus-induced IFN production has been facilitated by the availability of RIG-I$^{-/-}$ and MDA5$^{-/-}$ mice (34, 35). Both RLRs might be dominant receptors for RNA virus that result in the activation of innate immune systems, and initial observations using embryonic fibroblasts and bone marrow–derived dendritic cells generated from these mice revealed striking phenotypes, including a failure to produce IFN in response to a variety of viral infections (2, 5). Thus far, three families of PRRs, including RLRs, TLRs, and nucleotide-binding domain and leucine-rich-repeat-containing (NLR), have been identified and shown to be activated in response to IAV pathogens (36). The mechanism by which influenza viral infection triggers the secretion of NLR-induced inflammatory cytokines, such as IL-1β, IL-18, and IL-33, has been clearly reported, and we believe that NLRs might be closely related to inflammasome activation (36, 37). Therefore, we focused on the function of TLRs (TLR3, TLR7, TLR9) and RLRs (RIG-I, MDA5) in enhancing the innate immune response against IAV infection in NHNE cells and *in vivo* nasal mucosa.

Interestingly, we found that Duox2-derived ROS might be involved in RLR signaling to resist IAV infection in human nasal epithelia, and the induction of RIG-I and MDA5 transcription was dominant in mouse nasal mucosa after IAV inoculation. Most importantly, the IAV viral titer was markedly higher in the nasal mucosa or NAL fluid of shDuox2 mice than in shCont mice, and lowered induction of RIG-I and MDA5 expression was observed in the nasal mucosa of shDuox2 mice. Both RIG-I and MDA5 significantly contribute to the response to viral infection, and appear to be capable of producing IFNs; previously, we showed that intracellular Duox2-generated ROS contribute to type III IFN secretion against IAV infection in NHNE cells (14). Herein, we discern that Duox2 is primarily involved in the rapid induction of IAV recognition receptors, especially RIG-I and MDA5, and might initiate the innate immune response for the secondary control of IAV infection. A Duox2-mediated innate immune response would be expected if nasal epithelium frequently encounters various viruses, including IAV, and Duox2-derived ROS would be required for IAV sensing in human nasal epithelium or mouse nasal mucosa.

In previous studies, a role of ROS in RIG-I signaling in autophagy has been documented, and ROS were associated with RLR-mediated cytokine production (38, 39). It has not been clearly proven how ROS and Duox2 are responsible for the innate immune response in nasal epithelia, and we could not verify the concrete mechanism underlying the ROS-sensitive transcription of RIG-I and MDA5 in nasal epithelium. However, we propose a role for Duox2-derived ROS as a mediator of the antiviral defense mechanism in nasal epithelium, and that Duox2 might contribute to the activation of IFN-related innate immune signaling through the induction of cytoplasmic RLRs expression.

In conclusion, our study provides insight that Duox2-derived ROS may be crucial for the clearance of influenza virus in nasal epithelium. The absence of Duox2 leads to dysregulation of RIG-I and MDA5 expression and impedes efficient innate immunity, which aggravate IAV infection. ■

Author disclosures are available with the text of this article at www.atsjournals.org.

Figure 7. (Continued). mouse nasal mucosa. Western blot analysis was also performed using cell lysates to compare RIG-I and MDA5 protein expression levels at 7 dpi (*F*). shDuox2 mice ($n = 5$) were infected with 213 pfu IAV WSN/33 (H1N1) and were assessed for RIG-I and MDA5 mRNA levels using real-time PCR (*G*) and protein levels using western blot analysis (*H*) at 7 dpi. Western blot analysis results are representative of five mice, and PCR results are presented here as the mean ± SD from five independent experiments. $^*P < 0.05$ compared with levels in shCont mice and shDuox2 mice. PRR, pattern recognition receptor.

References

1. Kawai T, Akira S. Pathogen recognition with Toll-like receptors. *Curr Opin Immunol* 2005;17:338–344.
2. Yoneyama M, Kikuchi M, Natsukawa T, Shinobu N, Imaizumi T, Miyagishi M, Taira K, Akira S, Fujita T. The RNA helicase RIG-I has an essential function in double-stranded RNA-induced innate antiviral responses. *Nat Immunol* 2004;5:730–737.
3. Gitlin L, Benoit L, Song C, Cella M, Gilfillan S, Holtzman MJ, Colonna M. Melanoma differentiation–associated gene 5 (MDA5) is involved in the innate immune response to Paramyxoviridae infection *in vivo*. *PLoS Pathog* 2010;6:e1000734.
4. García-Sastre A, Biron CA. Type 1 interferons and the virus–host relationship: a lesson in détente. *Science* 2006;312:879–882.
5. Wu S, Metcalf JP, Wu W. Innate immune response to influenza virus. *Curr Opin Infect Dis* 2011;24:235–240.
6. Levy DE, Darnell JE Jr. Stats: transcriptional control and biological impact. *Nat Rev Mol Cell Biol* 2002;3:651–662.
7. Horimoto T, Kawaoka Y. Influenza: lessons from past pandemics, warnings from current incidents. *Nat Rev Microbiol* 2005;3:591–600.
8. Liu T, Castro S, Brasier AR, Jamaluddin M, Garofalo RP, Casola A. Reactive oxygen species mediate virus-induced STAT activation: role of tyrosine phosphatases. *J Biol Chem* 2004;279: 2461–2469.
9. van der Vliet A. NADPH oxidases in lung biology and pathology: host defense enzymes, and more. *Free Radic Biol Med* 2008;44:938–955.
10. Kim HJ, Kim CH, Ryu JH, Joo JH, Lee SN, Kim MJ, Lee JG, Bae YS, Yoon JH. Crosstalk between platelet-derived growth factor-induced Nox4 activation and MUC8 gene overexpression in human airway epithelial cells. *Free Radic Biol Med* 2011;50:1039–1052.
11. Haller O, Kochs G, Weber F. The interferon response circuit: induction and suppression by pathogenic viruses. *Virology* 2006;344:119–130.
12. Mellqvist UH, Hansson M, Brune M, Dahlgren C, Hermodsson S, Hellstrand K. Natural killer cell dysfunction and apoptosis induced by chronic myelogenous leukemia cells: role of reactive oxygen species and regulation by histiamine. *Blood* 1999;65:196–204.
13. Lipinski S, Till A, Sina C, Arlt A, Grasberger H, Schreiber S, Rosenstiel P. DUOX2-derived reactive oxygen species are effectors of NOD2-mediated antibacterial responses. *J Cell Sci* 2009;122:3522–3530.
14. Kim HJ, Kim CH, Ryu JH, Kim MJ, Park CY, Lee JM, Holtzman MJ, Yoon JH. Reactive oxygen species induce antiviral innate immune response through IFN-λ regulation in human nasal epithelial cells. *Am J Respir Cell Mol Biol* 2013;49:855–865.
15. Wang J, Oberley-Deegan R, Wang S, Nikrad M, Funk CJ, Hartshorn KL, Mason RJ. Differentiated human alveolar type II cells secrete antiviral IL-29 (IFN-lambda 1) in response to influenza A infection. *J Immunol* 2009;182:1296–1304.
16. Yoon JH, Gray T, Guzman K, Koo JS, Nettesheim P. Regulation of the secretory phenotype of human airway epithelium by retinoic acid, triiodothyronine, and extracellular matrix. *Am J Respir Cell Mol Biol* 1997;16:724–731.
17. Kim MJ, Ryu JC, Kwon Y, Lee S, Bae YS, Yoon JH, Ryu JH. Dual oxidase 2 in lung epithelia is essential for hyperoxia-induced acute lung injury in mice. *Antioxid Redox Signal* 2014;21:1803–1818.
18. Johnson KR, Marden CC, Ward-Bailey P, Gagnon LH, Bronson RT, Donahue LR. Congenital hypothyroidism, dwarfism, and hearing impairment caused by a missense mutation in the mouse dual oxidase 2 gene, Duox2. *Mol Endocrinol* 2007;21:1593–1602.
19. Rhee SG. Cell signaling. H_2O_2, a necessary evil for cell signaling. *Science* 2006;312:1882–1883.
20. Koarai A, Sugiura H, Yanagisawa S, Ichikawa T, Minakata Y, Matsunaga K, Hirano T, Akamatsu K, Ichinose M. Oxidative stress enhances Toll-like receptor 3 response to double-stranded RNA in airway epithelial cells. *Am J Respir Cell Mol Biol* 2010;42:651–660.
21. Vlahos R, Stambas J, Bozinovski S, Broughton BR, Drummond GR, Selemidis S. Inhibition of Nox2 oxidase activity ameliorates influenza A virus–induced lung inflammation. *PLoS Pathog* 2011;7:e1001271.
22. Vlahos R, Stambas J, Selemidis S. Suppressing production of reactive oxygen species (ROS) for influenza A virus therapy. *Trends Pharmacol Sci* 2012;33:3–8.
23. Pollock JD, Williams DA, Gifford MA, Li LL, Du X, Fisherman J, Orkin SH, Doerschuk CM, Dinauer MC. Mouse model of X-linked chronic granulomatous disease, an inherited defect in phagocyte superoxide production. *Nat Genet* 1995;9:202–209.
24. Gao XP, Standiford TJ, Rahman A, Newstead M, Holland SM, Dinauer MC, Liu QH, Malik AB. Role of NADPH oxidase in the mechanism of lung neutrophil sequestration and microvessel injury induced by Gram-negative sepsis: studies in p47phox$^{-/-}$ and gp91phox$^{-/-}$ mice. *J Immunol* 2002;168:3974–3982.
25. Zmijewski JW, Lorne E, Zhao X, Tsuruta Y, Sha Y, Liu G, Abraham E. Antiinflammatory effects of hydrogen peroxide in neutrophil activation and acute lung injury. *Am J Respir Crit Care Med* 2009; 179:694–704.
26. Bae YS, Choi MK, Lee WJ. Dual oxidase in mucosal immunity and host-microbe homeostasis. *Trends Immunol* 2010;31:278–287.
27. Park HS, Jin DK, Shin SM, Jang MK, Longo N, Park JW, Bae DS, Bae YS. Impaired generation of reactive oxygen species in leprechaunism through downregulation of Nox4. *Diabetes* 2005;54: 3175–3181.
28. Mahadev K, Motoshima H, Wu X, Ruddy JM, Arnold RS, Cheng G, Lambeth JD, Goldstein BJ. The NAD(P)H oxidase homolog Nox4 modulates insulin-stimulated generation of H_2O_2 and plays an integral role in insulin signal transduction. *Mol Cell Biol* 2004;24: 1844–1854.
29. Lambeth JD, Kawahara T, Diebold B. Regulation of Nox and Duox enzymatic activity and expression. *Free Radic Biol Med* 2007;43: 319–331.
30. Schwarzer C, Machen TE, Illek B, Fischer H. NADPH oxidase–dependent acid production in airway epithelial cells. *J Biol Chem* 2004;279: 36454–36461.
31. Ris-Stalpers C. Physiology and pathophysiology of the DUOXes. *Antioxid Redox Signal* 2006;8:1563–1572.
32. Weichart D, Gobom J, Klopfleisch S, Häsler R, Gustavsson N, Billmann S, Lehrach H, Seegert D, Schreiber S, Rosenstiel P. Analysis of NOD2-mediated proteome response to muramyl dipeptide in HEK293 cells. *J Biol Chem* 2006;281:2380–2389.
33. Snelgrove RJ, Edwards L, Rae AJ, Hussell T. An absence of reactive oxygen species improves the resolution of lung influenza infection. *Eur J Immunol* 2006;36:1364–1373.
34. Wies E, Wang MK, Maharaj NP, Chen K, Zhou S, Finberg RW, Gack MU. Dephosphorylation of the RNA sensors RIG-I and MDA5 by the phosphatase PP1 is essential for innate immune signaling. *Immunity* 2013;38:437–449.
35. Slater L, Bartlett NW, Haas JJ, Zhu J, Message SD, Walton RP, Sykes A, Dahdaleh S, Clarke DL, Belvisi MG, *et al*. Co-ordinated role of TLR3, RIG-I and MDA5 in the innate response to rhinovirus in bronchial epithelium. *PLoS Pathog* 2010;6: e1001178.
36. Allen IC, Scull MA, Moore CB, Holl EK, McElvania-TeKippe E, Taxman DJ, Guthrie EH, Pickles RJ, Ting JP. The NLRP3 inflammasome mediates in vivo innate immunity to influenza A virus through recognition of viral RNA. *Immunity* 2009;30:556–565.
37. Li H, Willingham SB, Ting JP, Re F. Cutting edge: inflammasome activation by alum and alum's adjuvant effect are mediated by NLRP3. *J Immunol* 2008;181:17–21.
38. Tal MC, Sasai M, Lee HK, Yordy B, Shadel GS, Iwasaki A. Absence of autophagy results in reactive oxygen species–dependent amplification of RLR signaling. *Proc Natl Acad Sci USA* 2009;106: 2770–2775.
39. Soucy-Faulkner A, Mukawera E, Fink K, Martel A, Jouan L, Nzengue Y, Lamarre D, Vande Velde C, Grandvaux N. Requirement of NOX2 and reactive oxygen species for efficient RIG-I–mediated antiviral response through regulation of MAVS expression. *PLoS Pathog* 2010;6:e1000930.